Effects of Grasp Frequency on the Dynamics of a Robotic Surgical Grasper[1]

Mark J. Brown
Department of Mechanical Engineering,
University of Minnesota,
Minneapolis, MN 55455

Trevor K. Stephens
Department of Mechanical Engineering,
University of Minnesota,
Minneapolis, MN 55455

John J. O'Neill
Department of Mechanical Engineering,
University of Minnesota,
Minneapolis, MN 55455

Timothy M. Kowalewski
Department of Mechanical Engineering,
University of Minnesota,
Minneapolis, MN 55455

1 Background

Endoscopic surgical instruments such as the da Vinci EndoWrist® are the interface between surgeon and patient in the burgeoning field of robotic surgery. In the current clinical setting, such tools are being used primarily as an extension of the surgeon's hands. However, more robust features such as online tissue identification may be integrated into the functionality of robotic surgical graspers in the future. For these applications, the tool dynamics should be well understood and modeled across a spectrum of frequencies. The linear model used to characterize the tool is a version proposed by Sie and Kowalewski [1] and is shown in Eq. (1). Refer to Ref. [1] for definition of model parameters

$$\theta_{ee} = K_1\ddot{\theta}_m + K_2\dot{\theta}_m + K_3\theta_m + K_4F_m \tag{1}$$

2 Methods

The robotic surgical grasper analyzed in this experiment was a modified da Vinci EndoWrist tool; the complete design is detailed in Ref. [2]. Grasping is actuated at the proximal end of the tool by two servomotors (Hitec-HS422) interfaced to the tool's spindles. Force data are acquired via two load cells (3132, Phidgets, Inc., Calgary, AB), each adjacent to a servo. Both load cells were calibrated by applying masses to each load cell in a cantilever arrangement and applying regression techniques. The tool was controlled by a microcontroller (mbed NXP LPC1768) with interrupt-capable communication for synchronization with the calibration testbed.

A novel calibration testbed was created to provide position data at the tool's end effector. Position was measured with two optical encoders (E5, U.S. Digital, Vancouver, WA). Quadrature encoding was implemented in code resulting in a resolution of 20,000 pulses per revolution at each encoder. Both optical encoder wheels were affixed to separate acrylic disks via a 3D printed spacer. A thin metal rod was inserted into each acrylic disk to allow the surgical tool's grasper to make normal contact with the acrylic disks and thus with the optical encoder wheel. The acrylic disks and encoder wheels were positioned in a uniaxial arrangement about a central steel rod with the use of small-diameter flanged ball bearings. Both rods were then placed in a lathe ensuring uniaxial alignment for the entire duration of testing. A torsion spring with constant $k = 1 \times 10^{-4}\text{N} \cdot \text{m/deg}$ was mounted onto the axle at each acrylic disk resulting in a grasping site that provided position data upon a known linear torque (Fig. 1).

The tool was placed into the calibration testbed and the end effector secured between the metal axles. The axis of rotation of the jaws was coincident with that of the axles. A frequency sweep was performed with a sampling rate of 1 kHz. Referring to Fig. 2, grasp frequency increased from 0.1 to 5.6 Hz in equally spaced logarithmic intervals. Typical surgical grasps are limited to 3 Hz [3]. Therefore, this range provided six equally spaced frequencies in the regime of typical surgical grasps as well as two frequencies above this typical threshold. Full range of angular motion of the grasping jaws was constrained to 60 deg, with 0 deg corresponding to the fully opened state. Five grasps were performed at each frequency resulting in a total of 40 measured grasps.

End-effector position data from the encoders were concatenated with the tool's position, force, and time data and imported into MATLAB (MathWorks, Inc., Natick, MA) for postprocessing. Position and force at the tool's servomotor were low-pass filtered using a fourth-order Butterworth infinite impulse response (IIR) filter. Applying the filter in postprocessing allowed for zero phase-shift filtering. Velocity and acceleration matrices of each grasp were obtained using robust numerical differentiation techniques proposed by Holoborodko [4]. Linear coefficients K_1, K_2, K_3, and K_4 were explicitly calculated using the entire matrices of proximal and end-effector data. The contribution of each individual coefficient with its respective state to the overall response $\theta_{ee,fitted}$ was then determined by numerical integration of each product $K_1\ddot{\theta}_m, K_2\dot{\theta}_m, K_3\theta_m$, and K_4Fm.

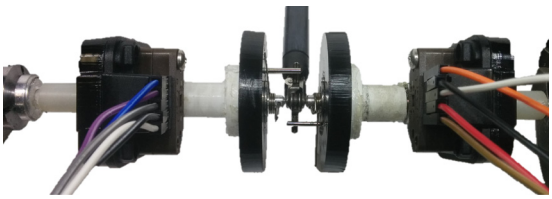

Fig. 1 Calibration testbed

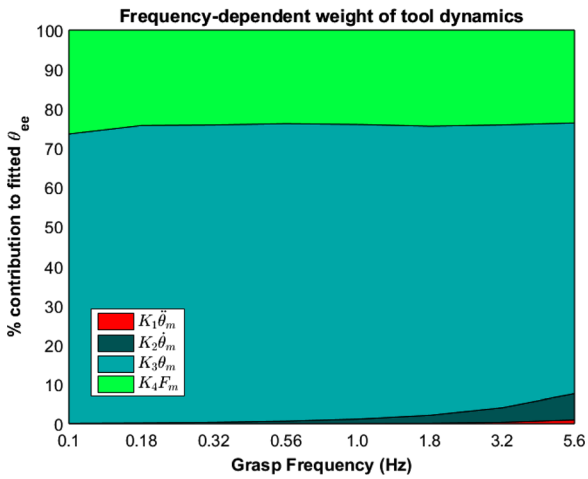

Fig. 2 The percent contribution to $\theta_{ee,fit}$

[1]Accepted and presented at The Design of Medical Devices Conference (DMD2016), April 11–14, 2016 Minneapolis, MN, USA.

DOI: 10.1115/1.4033844
Manuscript received March 1, 2016; final manuscript received March 17, 2016; published online August 1, 2016. Editor: William Durfee.

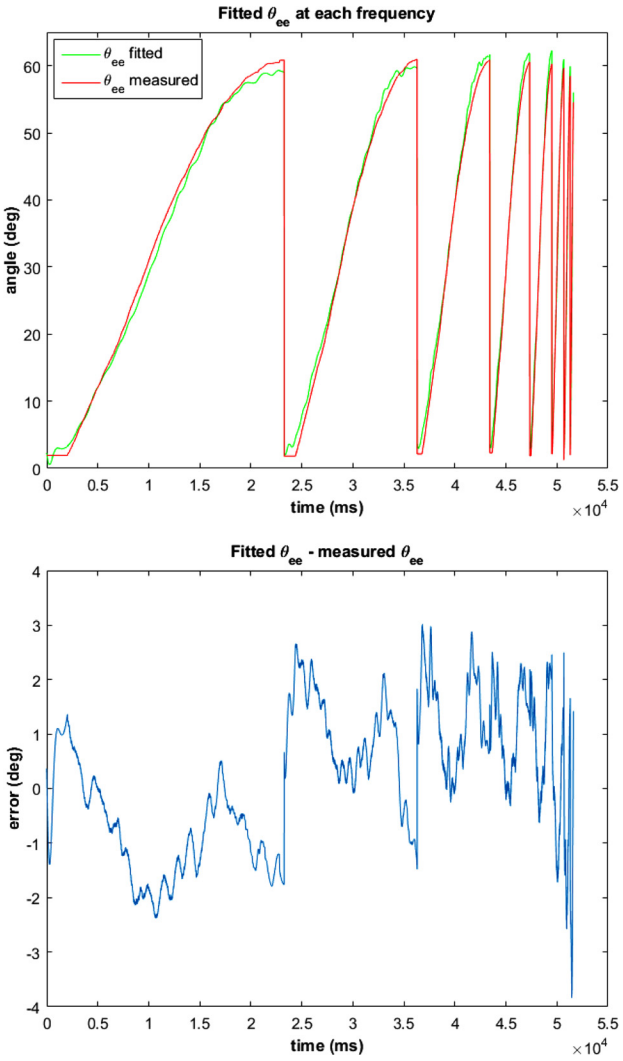

Fig. 3 Fit versus measured θ_{ee} (top) and error (bottom)

3 Results

The coefficient matrix from Eq. (1) (with units of s^2, s, l, and deg/N) was determined to be

$$[K_1 \;\; K_2 \;\; K_3 \;\; K_4] = [-2.34 \times 10^{-6} \;\; -3.58 \times 10^{-4} \;\; 1.36 \;\; -55.2] \tag{2}$$

A matrix of $\theta_{ee,fitted}$ was then obtained using Eqs. (1) and (2) with each parameter multiplied by its respective state. For confirmation of the fit, $\theta_{ee,fitted}$ was plotted with $\theta_{ee,measured}$ for one grasp at each frequency as shown in Fig. 3.

4 Interpretation

Figure 3 displays the fitted versus measured values of θ_{ee} for one grasp at each of the eight frequencies. The curve fit begins to worsen toward the peak of each grasp as the velocity of the end effector diminishes. This may imply that internal stiction of the tool is not ideally accounted for in the current dynamic model, and thus, the K_4F_m term could be improved. Beginning with the fourth frequency, θ_m fails to achieve the full 60 deg range of motion to which the servomotors are commanded.

Figure 2 displays the percent contribution of each dynamic term to that of $\theta_{ee,fitted}$. The K_1 and K_2 terms appear so small in relative magnitude as to be negligible. At a grasping frequency of 0.1 Hz, roughly 75% of $\theta_{ee,fitted}$ is due to $K_3\theta_m$ and 25% is due to K_4F_m. As frequency increases, the contribution of the force product decreases marginally. The velocity term increases steadily after 1 Hz reaching a percent contribution of approximately 5% at 5.6 Hz. The acceleration component is notably absent from frequencies below 3.2 Hz and has minimal presence at 5.6 Hz. This data suggest that the velocity component is minimal below grasping frequencies of 1 Hz and that the acceleration component is entirely negligible for frequencies below 5.6 Hz. At these low frequencies, Eq. (1) can be simplified to

$$\theta_{ee} = K_3\theta_m + K_4F_m \tag{3}$$

As reported by Brown et al., expert surgeons typically employ grasps below 3 Hz. Thus, in the regime below 3 Hz, the model for this tool would appear as Eq. (3). More research should be performed to determine the tool dynamics as they vary among surgical graspers for the determination of a more robust model.

References

[1] Sie, A., and Kowalewski, T. M., 2013. "Quantifying Forces at the Tool-Tissue Interface of a Surgical Laparoscopic Grasper," ASME J. Med. Devices, **7**(3), p. 030913.

[2] Stephens, T. K., Meier, Z. C., Sweet, R. M., and Kowalewski, T. M., 2015. "Tissue Identification Through Back End Sensing on da Vinci Endowrist Surgical Tool," ASME J. Med. Devices, **9**(3), p. 030939.

[3] Brown, J. D., Rosen, J., Kim, Y. S., Chang, L., Sinanan, M. N., and Hannaford, B., 2003, "In-Vivo and In-Situ Compressive Properties of Porcine Abdominal Soft Tissues," Stud. Health Technol. Inf., **94**, pp. 26–32.

[4] Holoborodko, P., 2016, "Smooth Noise Robust Differentiators," http://www.holoborodko.com/pavel/numericalmethods/numerical-derivative/smooth-low-noise-differentiators/